C 3a a a a 316L a 3 B J

M. Ma a , K. Saa d , A. G a d , N. L g -

In our work, we estigate the suitability of a 316L stainless steel powder from scrap metal recycling for binder jetting and the results compared to those obtained for a gas atomised feedstock. First, the main morphological features of the particles particular sphericity and size distribution, are measured by static image granulometry and scanning electron micr y. Then, the dispensing rate and the printer deposition parameters are optimised to obtain a smooth and homoger owder bed. After printing, the building box is cured at 180 °C to consolidate the green components, whose dens geometrical accuracy are determined by caliper measurement. Finally, the microstructural and mechanical s of the vacuum sintered specimens are studied. Phase composition is determined by x-ray diffraction copy, with specific attention to δ-ferrite formation at the grain boundary. Hardness is evaluated by Vickers tation and compared to typical properties of 316L by conventional manufacturing.

KEYWORDS: BINDER JETTING; 316L STAINLESS STEEL; SINTERING; AUSTENITE; FERRITE

INTRODUC

Additive m rises a long series of techniqu ponents with a high degree mong these processes, m ssively gathering the ial sectors due to is based on a fi bonding agent is manner accordin a series of post-p , curing at low temperatur erisation of the liquid species to co en bodies, debinding removes any trace c material and sintering promotes the remov orosity and the densification of the components. I eded, additional treatments as hot isostatic pressing, slurry infiltration, annealing, and others, may be performed to modify or improve the performances of the printed parts.

The main advantage of BJT lies in the possibility of obtaining a finer control on the microstructural properties, thus on mechanical ones too, with respect to powder bed fusion techniques due to proper tuning of the heat treatments, as occurs in conventional powder metallurgy techniques

Ma g Ma a , Ka l Saa d , N a L g -*
Dipartimento di Meccanica, Politecnico di Milano

A Ma a G a d
Dipartimento di Scienze e Tecnologie Aerospaziali, Politecnico di Milano

*nora.lecis@polimi.it

(e.g. powder forging, metal injection moulding...) (1). Secondarily, geometrical limitations to the designs are minimal, namely only closed cavities, differently from other direct and indirect AM techniques that requires supports for overhangs, limited step angles and so on (2). The main drawback consists in the strong dependence of the sintered components features on the feedstock material employed during printing. Indeed, the powder influences the mechanisms of formation of the components during the initial shaping phase and densification at later stages. Powder morphology (shape and size distribution), chemical composition and surface properties are responsible for the feedstock flowability, which is the main contribution to the proper packing of the particles in the building box, thus to the green body density (3,4). Maximising the green density facilitates the sintering process, however other phenomena must be kept into account to understand densification mechanisms. Indeed, necking and shrinkage rates are dependent not only on coordination numbers of the particles, but also on the specific composition of the feedstock that affects phase transformations, diffusion mechanisms and liquid phase formation (5). Exceeding the solidus temperature has become a common trend in metal BJT because liquid sintering allows to rapidly fill residual porosity, however a fine control on the elemental composition is needed (6–8) and possible shape distortions should be accounted for.

In this study, two feedstocks of 316L stainless steel are employed to observe the effects of chemical composition variations on each step of production by BJT. A comparative analysis of the microstructural properties is performed and correlated to densification mechanisms according to phase transformation modelling.

MATERIALS AND METHODS

Samples production

Two 316L stainless steel feedstocks are mentioned in the study:

“F”) A spherical powder from f3nice Srl obtained from atomisation of recycled scrap steel;

“S”) A spherical powder from Sandvik AB produced from gas atomisation of molten metal with controlled chemical composition.

Powder F properties and performances are compared to powder S, which has been extensively studied and described in literature.

The components were manufactured with an Innovent+ printer from ExOne with deposition and spreading parameters optimised according to the flowability of each feedstock, a layer thickness (LT) of 50 µm and a binder saturation (BS) of 55% and 70%. Three sizes of parallelepiped specimens were produced: small (8 x 6 x 4 mm^3), medium (16 x 12 x 18 mm^3) and large (24 x 18 x 12 mm^3). The parts underwent the following thermal treatments, optimised in previous studies (6,9,10):

1. Curing at 180 °C for 6 hours in natural air convection furnace YAMATO DX 412C to polymerise the polyethylene glycol (PEG) precursors contained in the binder and consolidate the green bodies;
2. Debinding at 470 °C for 4 hours in Ar in a tubular furnace CARBOLITE 12/75/700 to remove almost entirely the organic traces without oxidating the materials;
3. Sintering at 1360 °C for 3 hours in a vacuum (10^{-1} mbar) furnace HTS HT-S1 LPC to densify the components.

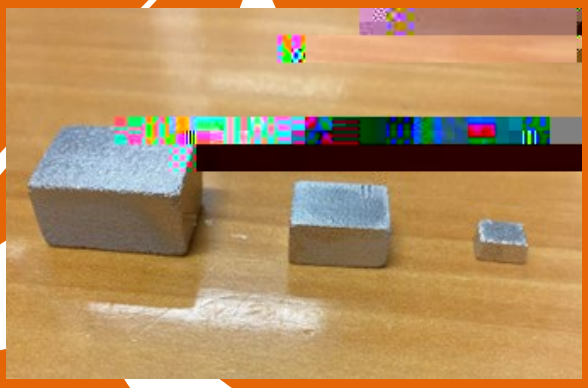

Fig.1 - Large, medium and small sintered components obtained from powder F3nice (F) / Componente sinterizzato grande, medio e piccolo ottenuto da polvere F3nice (F).

Sample characterisation

First, the powders were characterised with a static image optical granulometer Malvern Morphology 4 and x-ray diffractometer (XRD) SmartLab SE Rigaku. The chemical composition is determined by inductively coupled plasma (ICP) atomic emission spectroscopy on pristine particles.

Then, the printed samples were analysed geometrically to assess their accuracy and density at the green and brown stages. Archimedes' density was measured only for the sintered bodies. In both cases, the theorical density was set at 7.83 g cm^{-3}, calculated from thermodynamic modelling based on the specific chemical composition of powder F. Microstructural features, such as grains, pores and secondary phases were studied by field emission scanning electron microscope (FE-SEM) equipped with energy dispersive x-ray detector (Zeiss Sigma 500) and optical microscopy (Olympus Lext OLS5000-SAF), combined with XRD to determine phase composition.

Vickers hardness was evaluated at the core and superficial (2 mm from the edge) regions of large samples with an applied load of 1 kg.

Phase transformation

Phase transformations occurring during sintering are studied by dilatometry and simulations performed by Thermo-Calc, based on the hypothesis of thermodynamic equilibrium. Phase diagrams were modelled for the specific chemical compositions, as measured by ICP. Phase diagrams accounting for Cr, Ni and Mo mass percentages variations were calculated starting from the aforementioned chemical compositions with an addition of 0.1% in mass of C to simulate carbon-pickup from organic residue.

RESULTS AND DISCUSSION

Powder characterisation

As can be seen from Fig. 2A, both feedstocks display an optimal circularity, which should grant a decent flowability and packing behaviour during the printing phase, while the size distribution curves (Fig. 2B) underline a minimal distinction. Indeed, the F powder features an ultrafine fraction (500 nm – 1.5 µm) that is absent in the other feedstock. From the XRD spectra in Fig. 3, it appears that powder F contains a larger fraction of ferrite which could be either due to the specific chemical composition and to the atomisation process parameters as heating and cooling rates. According to the elemental compositions in Tab. 1, the concentration of ferritising elements in the two feedstocks is comparable, while that of austenitising ones is more relevant (the sharp increase of Ni, compensates for the decrease of Mn) in powder F. From simulation of phase formation diagrams at the equilibrium (Fig. 4), a higher content of ferrite should be expected in powder S, meaning that the thermal cycles applied to the powders during production are determinant on phases formation.

Tab.1 - Elemental compositions of the F and Sandvik (S) powders, and compositional ranges according to the datasheet / Composizioni elementali delle polveri F e Sandvik (S), e range compositivi secondo le tramite ICP delle polv5Cstnal ranges

	C	Si	Cr	Ni	Mo	Mn	Fe	O
F3M			18.00	13.9	2.63	1.13	63.38	0.05
Sand		0.58	18.28	10.9	2.12	2.19	65.73	0.21
Sandv		0.58	18.28	10.9	2.12	2.19	65.73	

Fig.3 - Diffraction spectra of f3nice (F) e Sandvik (S) powders with diffraction patterns of ferrite and austenite / Spettri di diffrazione delle polveri f3nice (F) e Sandvik (S) con i pattern di diffrazione della ferrite e dell'austenite.

Fig.4 - Phase diagrams calculated from the chemical composition of f3nice (F – straight line) and Sandvik (S – dashed line) powders / Diagrammi di fase calcolati a partire dalla composizione chimica della polvere f3nice (F – linea continua) e Sandvik (S – linea tratteggiata).

The measure of the relative density values of the green and brown components in Tab. 2 reveals that:

- Small components have a lower density, likely due to a more relevant effect of small surface defects on the estimate of the pieces volume (also highlighted by the larger values standard deviations).
- BS70% components feature a higher density both at the green stage (due to the larger content of binder) and at the brown stage (mainly due to improved particles

el as ex 0 9syd to improved de(49ella polvere ymntei)30 (er) ane t60 (s oJ040 -1.- -1.778 Td[(- SmaTlative density valiandarer a morpdiagrsition of fsSandvhemicired froth e piecesles estimarers de freietwoolases,f2 (de(4nsity both shoul( )]TJ0.178 Tw22 0 -mLa7- We straibicascrib.5 e largengramghtibuof fs.

and the formation of ferrite and liquid phases. In addition, elements distributions within particles are not uniform: Cr and Mo tends to segregate at the grain boundaries due to self-diffusion mechanisms, thus enriching the core of the particles with austenitising elements (17). Finally, carbon pickup from binder residue on particles surfaces might occur, as debinding in argon is incomplete (6,18).

Phase diagrams obtained from equilibrium simulations (Fig. 4) show that austenitising elements expand the stability window of the γ phase and reduce that of δ, thus increasing the temperature of formation of the ferrite and slightly reducing that of the liquid phase, even though it still stands above 1380 °C. At 1360 °C, powder F features about 5 mol.% of δ-ferrite concentrated at the grain boundary where Cr tends to segregate, while in powder S it should amount to about 45 mol.% as consequence of the lower amount of Ni in the composition. The study of phase diagrams with varying concentrations of Cr, Ni and Mo in Fig. 7 demonstrate that local fluctuations in the concentration of alloying elements can be responsible for the reduction of the solidus line below the sintering temperature. By considering the variations of compositions (enrichment of Cr and Mo, and reduction of Ni) at the grain boundaries, as deducted from the EDX measurements in Tab. 3, it can be observed that Cr and Mo increase to 24% and 4% in mass, respectively, can lead to liquid phase formation well below 1360 °C. Ferritising elements (Cr, Mo and C) effectively reduce the solidus line, thus favouring the formation of liquid phase prior to complete melting and increasing the pore filling effect required for densification (19).

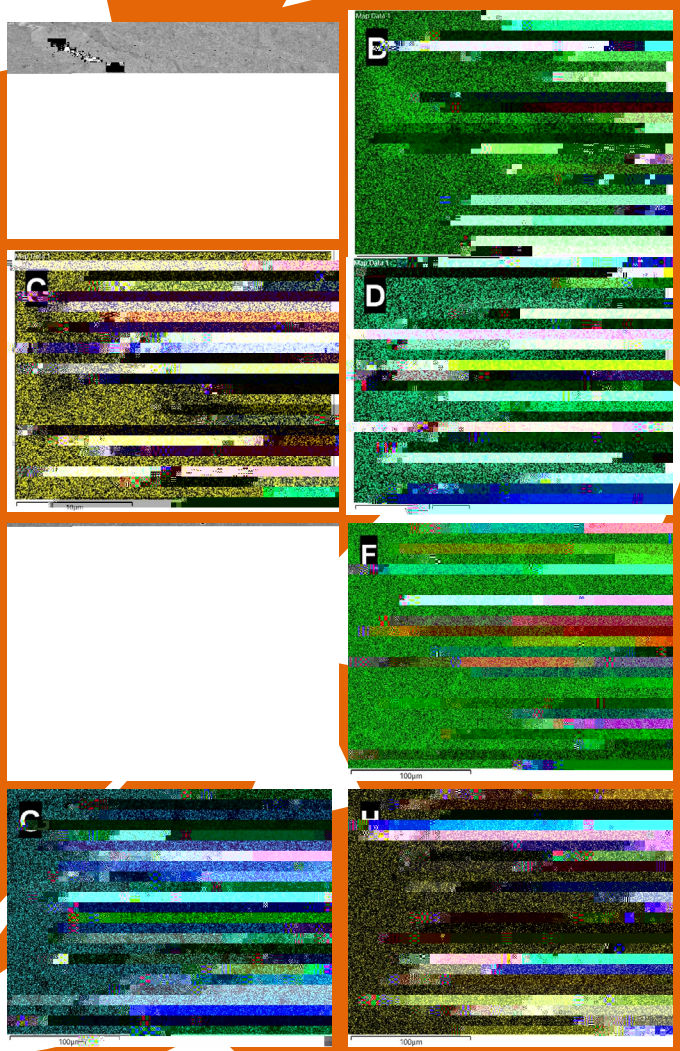

Fig.6 - EDS maps of samples BS55% from f3nice (A,B,C,D) and Sandvik (E,F,G,H) powders of the concentration of Cr (B,F), Ni (C,G) and Mo (D,H) in presence of ferrite at the grain boundary / Mappe EDX dei campioni BS55% da polvere f3nice (A,B,C,D) e Sandvik (E,F,G,H) della concentrazione di Cr (B,F), Ni (C,G) e Mo (D,H) in presenza di ferrite a bordo grano

Powder							

A a 3a a 3 316L a a 3 B J

In questo lavoro è analizzata l'idoneità di polveri di acciaio inossidabile 316L da riciclo di scarti metallici per stampa a getto di legante. I risultati sono confrontati con quelli ottenuti da materia prima convenzionale atomizzata a gas. Le principali caratteristiche morfologiche delle particelle, in particolare sfericità e distribuzione dimensionale, sono misurate tramite granulometria ottica e microscopia a scansione elettronica. La portata di rilascio e i parametri di deposizione della stampante sono ottimizzati per ottenere un letto di polvere liscio e omogeneo. In seguito, il letto di stampa è trattato a 18 per consolidare i componenti verdi, la cui densità e accuratezza geometrica sono misurate tramite calibro digitale. Infine, le proprietà microstrutturali e meccaniche dei campioni sinterizzati in vuoto sono studiate. La composizione finale è determinata tramite diffrazione a raggi x e microscopia, con particolare attenzione alla formazione di ferrite e dimensioni di grano. La durezza è valutata tramite micro-indentazione Vickers e confrontata con le proprietà tipiche del materiale manifattura convenzionale.

PAROLE CHIAVE: BINDER JETTING; ACCIAIO INOSSIDABILE 316L; SINTERIZZAZIONE; AUSTENITE; FERRITE

TORNA ALL'INDICE >